The collection of MicroED data for macromolecular crystallography

Dan Shi[1], Brent L Nannenga[1], M Jason de la Cruz[1], Jinyang Liu[1], Steven Sawtelle[1], Guillermo Calero[2], Francis E Reyes[1], Johan Hattne[1] & Tamir Gonen[1]

[1]Janelia Research Campus, Howard Hughes Medical Institute, Ashburn, Virginia, USA. [2]Department of Structural Biology, University of Pittsburgh School of Medicine, Pittsburgh, Pennsylvania, USA. Correspondence should be addressed to T.G. (gonent@janelia.hhmi.org).

Published online 14 April 2016; doi:10.1038/nprot.2016.046

The formation of large, well-ordered crystals for crystallographic experiments remains a crucial bottleneck to the structural understanding of many important biological systems. To help alleviate this problem in crystallography, we have developed the MicroED method for the collection of electron diffraction data from 3D microcrystals and nanocrystals of radiation-sensitive biological material. In this approach, liquid solutions containing protein microcrystals are deposited on carbon-coated electron microscopy grids and are vitrified by plunging them into liquid ethane. MicroED data are collected for each selected crystal using cryo-electron microscopy, in which the crystal is diffracted using very few electrons as the stage is continuously rotated. This protocol gives advice on how to identify microcrystals by light microscopy or by negative-stain electron microscopy in samples obtained from standard protein crystallization experiments. The protocol also includes information about custom-designed equipment for controlling crystal rotation and software for recording experimental parameters in diffraction image metadata. Identifying microcrystals, preparing samples and setting up the microscope for diffraction data collection take approximately half an hour for each step. Screening microcrystals for quality diffraction takes roughly an hour, and the collection of a single data set is ~10 min in duration. Complete data sets and resulting high-resolution structures can be obtained from a single crystal or by merging data from multiple crystals.

INTRODUCTION

The need to obtain large crystals for high-resolution structure determination by X-ray crystallography is often prohibitive for many difficult yet important samples. This has led structural biologists to look toward new methods and equipment, such as X-ray free-electron lasers (XFELs)[1] and microfocus beamlines[2], that are capable of providing structural data from microcrystals that are too small for conventional crystallography. MicroED is a recently developed method[3,4], which allows the collection of high-resolution electron diffraction data from extremely small protein microcrystals using an electron cryo-microscope (cryo-EM). Similar techniques have been developed in material science for beam/dose insensitive inorganic and small organic molecule electron diffraction under noncryogenic conditions (e.g., electron diffraction tomography and rotation electron diffraction)[5–9]. MicroED has thus far yielded high-resolution structures of several model proteins[3,4,10–12], as well as two novel structures of the toxic core of α-synuclein at 1.4 Å resolution, a sample that resisted structure determination by other methods for many years until MicroED was successfully used[11] (**Fig. 1**).

The MicroED method is ideal when crystallization experiments produce crystals that are thinner than ~400 nm (larger and thicker crystals can be studied by traditional X-ray crystallography). Although crystals in this size range could possibly also work for XFEL methods, there are advantages to using MicroED. In XFEL experiments, hundreds of micrograms to hundreds of milligrams of crystals are needed, as a jet of crystals is streamed into the diffracting beam[1,13–15]. In sharp contrast, in MicroED, a single nanocrystal can be sufficient for an entire data set[3,10], whereas for lower symmetries multiple data sets from a handful of crystals can be merged together[11]. While in XFELs such merged data sets can contain 1,000 individual still diffraction images hand-picked from a collection of 1,000,000 diffraction patterns, in MicroED only 1–3 crystals are often necessary for a complete data set to be obtained. This is because in MicroED crystals last long enough in the electron beam to allow a rotation series to be collected, which also results in the recording of full reflection intensities rather than the partials recorded in XFELs[3]. As such, fewer crystals are needed, and the indexing, merging integration and scaling are more straightforward than in XFEL experiments. Finally, for MicroED, standard equipment that is available at many universities and research institutes around the world is required while XFELs are scarce and beam time is limiting.

Further development of software for processing MicroED data is necessary. A general limitation of crystallographic software is that electron-scattering factors are not described accurately. Therefore, data analysis often results in excellent merging and integration statistics, and structure analysis yields quality density maps, but the R factors (a measure of the agreement between the data and the model) are typically relatively high. (This is also typically the case for XFEL data sets, although for reasons that are not well understood.) Efforts at calculating and integrating the correct scattering factors for electrons are currently underway and involve multiple laboratories.

For MicroED, samples are prepared by depositing microcrystals in solution on a carbon-coated EM grid, followed by solution removal by blotting and vitrification by plunge-freezing in liquid ethane or liquid nitrogen. Diffraction data are collected on a complementary metal-oxide-semiconductor (CMOS)–based detector, in a standard cryo-EM. Other detectors may be used; however, as the stage continues to rotate even as the detector is inactivated during readout, it is crucial that the frame rate be fast enough such that significant portions of data are not left unrecorded. Generally, CCDs are not recommended, as they tend to be slow, they have limited dynamic range and overexposure

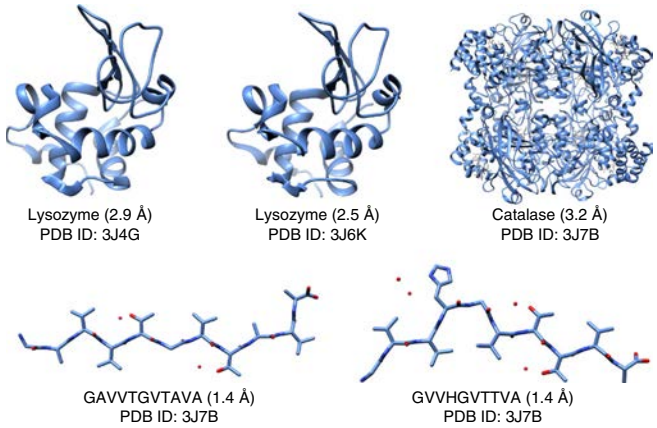

Figure 1 | Structures determined by MicroED. The proteins solved by MicroED are shown along with their Protein Data Bank (PDB) IDs and the final resolutions of the resulting structures.

(when a diffraction spot may overload the sensitivity of the sensor) may result in blooming effects where the signal 'bleeds' onto neighboring pixels. This 'bleeding' effect is greatly reduced in CMOS-based cameras such as the TVIPS F416. Direct electron detectors, such as the Gatan K2, could also be used, although special care needs to be taken to prevent sensor damage from the incident beam. To our knowledge, the FEI falcon camera cannot be used when the microscope is in diffraction mode, because the beam cannot be unblanked while their camera is in use to prevent damage to the sensor, suggesting that the manufacturer does not recommend the use of this camera for MicroED. Although many different detectors can be used, we recommend the CMOS-based TVIPS F416, as it has high sensitivity, high dynamic range and no 'bleeding' into neighboring pixels. These features make the F416 ideal for MicroED data collection. The microscope is operated in low-dose mode (low number of electrons per Å^2 per second) to limit the sample's exposure to damaging radiation, and it is similar to the EM setup used for 2D electron crystallography[16]. Within the low-dose settings, we use the search mode for low-magnification screening of the entire grid. Focus mode is used as a local search mode at higher magnification to identify and center suitable crystals within the beam and selected area (SA) aperture. Exposure mode is used for dose rate calibration, as well as for diffraction data collection.

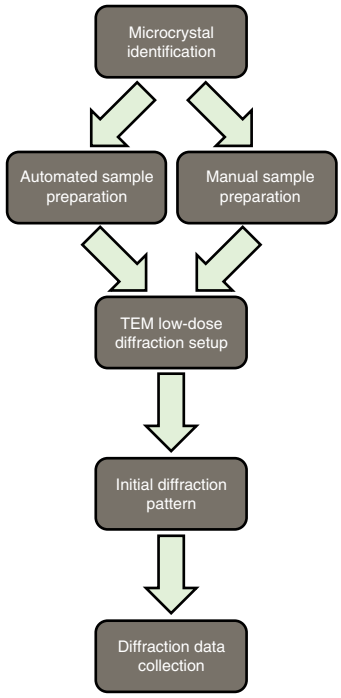

Figure 2 | Flow diagram for MicroED data collection protocol. The protocol begins with identifying suitable microcrystals using light microscopy and then preparing frozen samples by either automated vitrification systems or manual methods. After the microscope has been set up for low-dose diffraction and microcrystals identified on the grid, initial diffraction patterns are collected to assess crystal quality. When a high-quality crystal is found, diffraction data sets are collected[4].

Here we present a detailed protocol for microcrystal identification, sample preparation, cryo-EM setup for low-dose diffraction and MicroED data collection (**Fig. 2**). It is important that the experimenter be familiar with the setup and operation of transmission electron microscopes. After data collection, the data can be processed using standard programs for X-ray crystallography, such as MOSFLM[17,18], XDS[19], the HKL suite[20], DIALS[21], CNS[22,23], PHENIX[24], Buster[25], SHELX[26] and the CCP4 suite[27], and high-resolution structures can be determined as described in previous work[10,28]. Details of data processing have been published recently[29] and should be combined with this detailed protocol for data collection.

MATERIALS

REAGENTS

- Uranyl formate, 0.75% (wt/vol; SPI supplies, cat. no. 02545-AA; see Nannenga *et al.*[30] for solution preparation)
- Liquid nitrogen
- Liquid ethane

Protein sample (see Reagent Setup for further information)

EQUIPMENT

- 300-Mesh copper holey carbon or continuous carbon EM grids (Quantifoil micromachined holey carbon grids, SPI Supplies)
- Glow discharge cleaning system (PELCO easiGlow, Ted Pella)
- Pipetting device capable of pipetting 1- to 10-µl volumes
- Filter paper (Ted Pella, Grade 595 for Vitrobot blotting, Whatman no. 1 for manual blotting)
- Anticapillary reverse (self-closing) tweezers
- Plunge-freezer (FEI Vitrobot, Leica EM GP, Gatan CP3) for automated vitrification
- Locking tweezers assembly
- Cryo-grid storage boxes
- Cryo-EM with high-tilt stage
- High-tilt cryo-transfer holders such as Gatan 626 holder
- Complementary metal-oxide-semiconductor (CMOS)–based EM camera, such as the TVIPS TemCam-F416 (see INTRODUCTION for more information about different detectors)
- Gatan cryo-holder pumping station

REAGENT SETUP

Microcrystals Microcrystals of biological material are prepared by standard macromolecular crystallization procedures. Generally our laboratory uses hanging-drop vapor diffusion; however, sitting drop, liquid-liquid diffusion

Box 1 | Controlling stage rotation

The rotation of the stage during data collection can be controlled manually (α-tilt on the control panel), through software or through an external device. We designed and built an external device that uses a potentiometer to simulate the control panel's piezo sensor in order to generate an adjustable electric voltage signal to control the tilting rate of the compustage. The potentiometer (CW) output signal controls tilt speed. The two red boxes are switches for controlling main power and tilt direction.

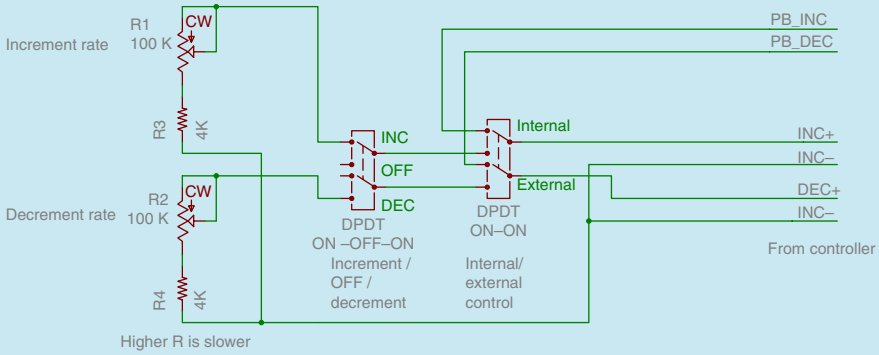

and batch crystallization have also been used. Crystallization conditions with extremely viscous components (e.g., high concentrations of glycerol or high-molecular-weight PEGs) may cause problems with sample preparation, as they can hinder blotting and grid preparation. Cryo-protection is typically not necessary, as the samples are embedded in vitrified ice.

EQUIPMENT SETUP

Constant rotation controlling device For MicroED, the standard transmission electron microscopy (TEM) equipment is used. The only meaningful modification that we have made was to build a constant rotation controlling device that is described in this protocol (**Box 1**). The normal operating control uses pressure-sensitive resistors to provide manual control. The adapter brings those control signals out to an external enclosure. When the internal/external switch is in the internal mode, it allows the operator to operate the system normally by feeding the pressure-sensitive resistor signals back into the increment/decrement circuits. When the switch is in external mode, standard potentiometers are switched into the circuit in lieu of the pressure-sensitive controls. There are separate controls for increment and decrement rates so that they can be adjusted independently. The setting of each potentiometer mimics a constant pressure on the built-in control. The increment/off/decrement switch only allows one (or neither) of the potentiometers to be connected to the circuit so that it can be used to allow movement in one direction or the other (or stop) at the rate determined by the appropriate potentiometer setting.

Calibrating the electron dose of the microscope It is important that the dose rate of the microscope be calibrated. If the dose rate of the microscope has not been calibrated, it can be done by first finding an open space, such as an area of carbon with no crystals or large area of broken carbon film, while in exposure/bright field mode. Record a 10-s exposure and use the CMOS camera counting rate to measure the dose rate in $e^-/Å^2/s$. The CMOS camera must first be calibrated according to the manufacturer's specifications by using a Faraday cage together with the microscope's phosphor viewing screen to allow the counting rate to be properly converted to dose rate.

PROCEDURE

Identification of microcrystals

1| Identify potential microcrystals by light microscopy. UV microscopy can also be used to help discriminate protein crystals from salt crystals that arise from the crystallization buffers (protein crystals will generally fluoresce while salt will not), although it can give false positives when protein aggregates surround salt crystals or when lipids and detergent crystals are present and contain minor amounts of integrated protein. Second-order nonlinear imaging of chiral crystals (SONICC) is an additional technique that could be useful for distinguishing between extremely small protein (chiral) and inorganic (generally achiral) crystals[31], although here again false positives are often encountered and the technology struggles with certain crystal packing symmetries. Refer to **Figure 3** for example microcrystal images from a light microscope. If potential microcrystal hits are found, they can be further screened by negative stain (see Steps 2–8 below) or even by collecting powder X-ray diffraction from the microcrystalline sample. Negative staining with uranyl formate is useful because protein crystals can be directly identified when the lattice is imaged. X-ray powder diffraction can help identify protein crystals and give an indication of crystal order. However, if the number of crystals in the drop is low, the signal in the powder diffraction may be very weak. Well-characterized samples may be immediately prepared for cryo-EM (Step 9).

2| *Negative staining (Steps 2–8)*. Clean the surface of holey carbon or continuous-carbon TEM grids by placing them carbon-side up in a glow-discharge plasma cleaning system. Activate glow-discharge on the grids for 30 s at 15 mA current with negative polarity.

3| Grip a freshly glow-discharged carbon-coated TEM grid in a pair of reverse tweezers. Deposit 1–4 µl of the microcrystal sample onto the grid. Let the crystals rest on the grid for 30 s.

4| Remove excess solution by touching the side of the grid to Whatman no. 1 filter paper.

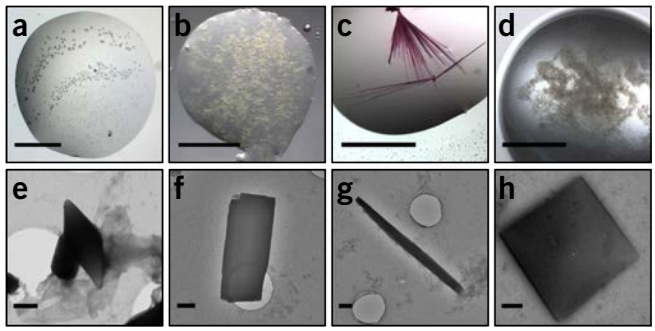

Figure 3 | Representative protein microcrystal images. Crystallization conditions that produce microcrystals can be identified by light microscopy in cases. Shown are examples in which small crystals are visible in light microscopy (**a**–**c**) and their corresponding images in negative-stain electron microscopy (EM; **e**–**g**), as well as an example in which only granular aggregates are observed by light microscopy (**d**), but the sample contains nanocrystals when investigated by EM (**h**). Scale bar, 500 nm (in **a**–**d**) and 400 nm (in **e**–**h**).

5| Immediately apply 3 µl of 0.75% (wt/vol) uranyl formate negative-stain solution to the grid and quickly blot off the uranyl formate solution with the Whatman no. 1 filter paper.

6| Again, apply 3 µl of 0.75% (wt/vol) uranyl formate negative-stain solution to the grid. Let the staining solution sit on the grid for 20 s.

7| Blot off the uranyl formate solution with the Whatman no. 1 filter paper until the sample is completely dry.

8| Load the stained EM grid into an electron microscope and screen the grid for microcrystals. Examples of negatively stained microcrystals visualized in EM can be seen in **Figure 3**. Additional examples can be found in Stevenson *et al.*[32].

Sample preparation for MicroED

9| Clean the surface of holey carbon or continuous-carbon EM grids (we typically use 300-mesh copper Quantifoil grids for MicroED) as described in Step 2. If the sample will be deposited on both sides of the grid (see troubleshooting tips in **Table 1**), flip grids over and glow-discharge again with the same settings.

? TROUBLESHOOTING

10| Option A describes the steps for blotting and freezing the sample using an automated vitrification apparatus (e.g., FEI Vitrobot, Leica EM GP, Gatan CP3). This option provides better control over the blotting conditions and improved reproducibility when compared with manual blotting. Generally, this is the first option used for sample preparation; however, this procedure can result in fewer microcrystals seen on the grid. This is because the blotting paper comes in direct contact with the solution sitting on the grid, and the fluid flow can carry crystals away from the carbon surface.

Option B describes the steps for blotting and freezing samples manually. This option is normally used either when the microcrystal concentration is lower (as it attempts to direct crystals toward the grid surface) or when the viscosity of the solution is high such that automated blotting systems are unable to remove enough sample buffer.

(A) Automated vitrification with Vitrobot

(i) Attach fresh Grade 595 filter paper to the blotting pads in the Vitrobot.

(ii) Set the desired temperature and humidity. Generally, room temperature (of ~17 °C) and 50% humidity are good starting points; however, these parameters can be optimized for each sample based on how thick the ice is for each grid.

(iii) Assemble the coolant container as shown in **Figure 4**. Place a cryo-gridbox into the box holder, and fill the outer reservoir with liquid nitrogen.

(iv) When the temperature of the liquid nitrogen has stabilized, slowly fill the inner brass reservoir with ethane. The low temperature of the brass reservoir will cause the ethane to condense. It is important to have the aluminum bridge present to transfer the heat from the condensing ethane into the liquid nitrogen reservoir. When you are done adding liquid ethane, remove the aluminum bridge and place the ethane container in the Vitrobot.

! CAUTION Liquid ethane is explosive; handle it with care. When you are finished making samples, allow the liquid ethane to evaporate in a chemical fume hood.

▲ CRITICAL STEP In the following steps, ensure that the level of liquid nitrogen in the reservoir does not fall below the top of the cryo-gridbox. Fill the reservoir with additional liquid nitrogen as needed.

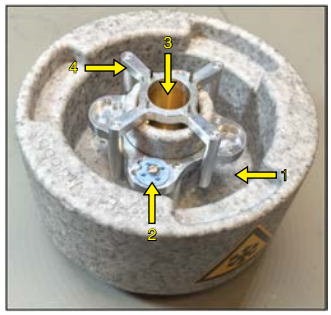

Figure 4 | Assembled Vitrobot coolant container. Before liquid nitrogen is added to the coolant container outer reservoir (1), as described in Step 10A(iii), the cryo-gridbox (2), inner brass ethane container (3) and aluminum bridge (4) should be properly assembled, as shown above.

(v) Grasp a freshly glow-discharged grid with a pair of locking tweezers. Gently pipette 4 µl of the microcrystal solution onto the carbon surface of the grid. Alternatively, 2 µl of solution can be added to each side of the grid.

(vi) Mount the tweezers assembly by holding the grid with microcrystal solution onto the tweezers rod of the Vitrobot. Select blotting force and blotting time and then process the sample. A blotting force of 1 is a good starting point, and it is recommended that multiple samples should be made with a wide range (2–12 s) of blotting times in order to determine the optimal ice thickness.

▲ **CRITICAL STEP** Enough solution needs to be removed so that the electron beam can penetrate the sample; however, excessive drying of the crystals should be avoided. Finding the optimal blotting time is a trial-and-error process.

(vii) After the sample has been plunged into the liquid ethane, remove the tweezers assembly and quickly move the sample from the liquid ethane into the liquid nitrogen in the outer reservoir. Load the grid into the cryo-gridbox.

(viii) Repeat Step 10A(v–vii) for each additional sample.

■ **PAUSE POINT** Grids may be examined in the microscope immediately after they are prepared. Alternatively, they may be stored in liquid nitrogen indefinitely.

(B) Blotting and freezing samples manually

(i) Prepare the coolant container and add the crystal solution to one side of a freshly glow-discharged grid as described in Step 10A(iii–v), but place the ethane container on a bench, preferably in a fume hood, instead of loading it in the Vitrobot.

(ii) Blot the crystal solution by touching the back of the grid to Whatman no. 1 filter paper and letting the crystal solution flow slowly through the grid to the filter paper.

(iii) When the solution has been removed, quickly freeze it in the liquid ethane followed by loading into the cryo-gridbox under liquid nitrogen in the outer reservoir.

(iv) Repeat Step 10B(i–iii) for each additional sample.

■ **PAUSE POINT** Grids may be examined in the microscope immediately after they are prepared. Alternatively, they may be stored in liquid nitrogen indefinitely.

Setting up the TEM for low-dose electron diffraction (FEI Tecnai series)

11| Load the frozen sample into the microscope using a cryo-transfer holder. A protocol for loading vitrified cryo-TEM samples can be found in Grassucci *et al.*[33]; this is also available in PubMed Central http://www.ncbi.nlm.nih.gov/pmc/articles/PMC2654234/.

12| While the microscope is in imaging mode, use the *Z*-height adjustment to accurately set the eucentric height. This can also be done while the microscope is in overfocused diffraction mode instead of imaging mode. First, use the microscopes wobbler function to roughly set the eucentric height. Next, find a defining feature on the grid such as a hole, a black blob, thick ice or grid edge (anything distinguishable from background will work), and then move it to the center of the screen and tilt the stage from 0° to 30–60°. Re-center the feature using the *Z*-height adjust button, and return the stage back to 0°. Move the feature back to the center of the screen using *X*,*Y* stage positioning, and repeat this step on the same feature until the feature stays centered while moving from 0° to high tilt angles (**Fig. 5**).

▲ **CRITICAL STEP** Accurate setting of the eucentric height is crucial for all subsequent steps in the PROCEDURE.

13| Move to an empty region of the carbon film, adjust the magnification in the SA range (defined by the manufacturer; 1,700× or higher depending on microscope configuration) and focus the image of carbon film accurately.

14| LM, like SA, is set by the manufacturer; it is displayed on the magnification range of the FEI microscopes computer. To set up low-dose mode (**Fig. 6**), which consists of search, focus and exposure settings, first activate low-dose mode from the computer interface. To set up the search mode, activate 'search', decrease magnification to LM mode and adjust the spot size to 10.

15| Align the beam center for the focus and exposure modes by first selecting 'focus' and then changing spot size to spot size 11 and magnification to the SA range. Set the focus shift distance to 0 µm, adjust the intensity such that the beam is visible on the screen and then center the beam using beam shift. Next, shift to exposure mode by selecting 'Exposure'. Again, set the spot size to 11, adjust

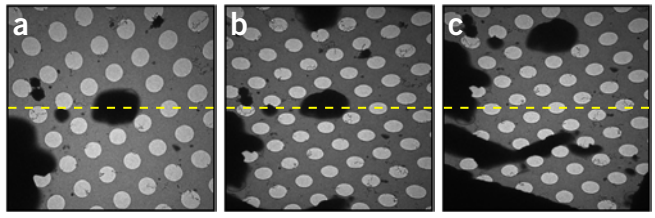

Figure 5 | Setting the eucentric height correctly. When the eucentric height has been set properly, features at the center of the screen do not move when the microscope is tilted. (**a**,**b**) The crystal seen at the center of the untilted sample (**a**) remains centered after the stage is tilted when the eucentric height is set correctly (**b**). (**c**) If the eucentric height is not set correctly (+16 µm in this example), the crystal swings away from the image center during tilting. The dashed yellow line indicates the tilt axis.

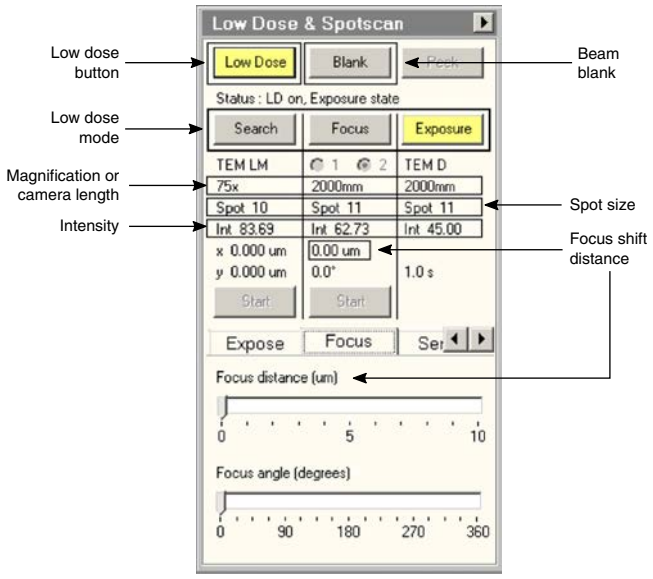

Figure 6 | Low-dose settings menu on the FEI Tecnai F20 microscope. Screenshot showing representative low-dose settings used during MicroED data collection. The microscope is currently in exposure mode, which is indicated by 'Exposure' being highlighted in yellow.

the intensity such that beam is visible on the screen and center the beam. Shift back and forth between focus and exposure modes, recentering the beam each time using the beam shift controls. Repeat until the beam stays centered after alternating between the two modes.

▲ **CRITICAL STEP** This process helps correct any electronic hysteresis. If hysteresis is not corrected, the electron optics will not be stable and targets on the grid may drift in and out of the beam. This may result in crystals drifting out of the diffracting beam during the experiment.

16| Set the desired dose rate by adjusting the intensity. The standard rate used for microcrystal diffraction is ~0.0.1 $e^-/Å^2/s$. See Equipment Setup for dose rate calibration.

17| Use the control panel to put the microscope into diffraction mode and then shift to focus mode. Expand the beam size 4–8 times larger than the exposure mode by decreasing the intensity (over-focusing C2 lens). Note that as the intensity is decreased the C2 lens power value displayed in the low-dose menu (**Fig. 6**) will increase. This means that while the actual intensity in focus mode is lower than in exposure mode, the intensity value displayed in the menu will be higher for focus mode. Focus mode will be used for local searching and centering crystals before exposure.

18| To center the SA aperture, overfocus the diffraction pattern in exposure mode (using the focus control knob on the control panel) and find a defining feature on the grid. Move the stage such that the feature is at the center of the image. Insert the SA aperture and adjust it such that it is centered over the feature on the grid.

19| Use the magnification controls to set the desired detector distance. The optimal detector distance should be close enough to capture all of the high-resolution data, yet far enough away to keep the diffraction spots well separated. See **Box 2** for information regarding the calibration of the detector distance.

20| Using the small phosphor screen, focus the center spot in exposure mode using the focus knobs such that it has the sharpest and the smallest diameter possible. If it is not possible to make the beam very sharp and the shape of the beam is more elongated than circular, see **Box 3** for how to check for and correct any astigmatism.

Box 2 | Calibrating detector distance

Because every microscope and camera system is unique, the detector distance must be calibrated. To do this, TEM grids with standard samples are loaded into the microscope and diffraction data are collected with the same settings as used in Step 19. Combined TEM test specimen—gold/graphitized carbon grids (Ted Pella, prod. no. 638)—can be used to calibrate detector distances that yield maximum obtainable resolutions higher than 3.4 Å. First, the diffraction pattern of the sample is collected at the desired detector distance, and then the following formula is used:

$$L\lambda \approx Rd$$

where L is the calibrated virtual detector distance, λ is the relativistic wavelength of the electrons (0.0251 Å for 200 kV acceleration voltage), R is the radius of the diffraction ring (calculated by measuring the radius of the ring in pixels and multiplying it by the pixel size of the detector) and d is the known lattice spacing. The Gold (111) lattice spacing will produce a characteristic diffraction ring at 2.35 Å, and the graphite will produce a ring at 3.4 Å. Record diffraction patterns of Au/graphite at the detector distances to be used for data collection.

Calibration can also be performed using test grids of well-known protein nano-crystals with larger unit cells (e.g., catalase crystals, Electron Microscopy Sciences). For these calibration standards, the known lattice parameters and the distances between Bragg reflections are used to calibrate the detector distance.

Box 3 | Correcting astigmatism of diffraction lens

If the beam appears to suffer from significant astigmatism, it can be corrected by first either removing the sample or moving to an area of the grid with broken carbon. Next, overfocus the condenser lens 2 (Tecnai F20 C2 at about 55% power or higher) and set the camera length to 3 m while in diffraction mode. Refer to the microscope manufacturer's user manual to correct for any astigmatism using the diffraction stigmators. After astigmatism has been properly corrected, the beam should appear as a sharp spot in the center of a three-pointed star when the diffraction pattern is slightly overfocused. Astigmatism correction should be very stable as long as the microscope settings remain constant.

21| Insert the beam stop and move it to the detector center. Use the diffraction shift controls to shift the direct beam so that it is completely blocked by the beam stop. It is important that the direct beam be blocked by the beam stop to prevent damage to the detector. The microscope is now set up to collect diffraction data.

Microcrystal diffraction and collection of diffraction data sets

22| Put the microscope in search mode and survey the quality of the grid and identify regions of interest. Good areas of the grid must have thin ice and well-separated microcrystals (**Fig. 6a**).

23| Go to a region of interest identified in search mode, and put the microscope in focus mode. Search the area for microcrystals and identify suitable crystals.

24| When a suitable crystal is found (**Fig. 7**), insert the SA aperture and center the crystal inside it. Accurately adjust the eucentric height as described in Step 12. The crystal should remain inside the SA aperture throughout the desired tilt range.

25| Insert the beam stop. After blanking the beam using the beam blank function, switch the microscope to exposure mode.

26| Unblank the beam and take an initial diffraction pattern with an exposure of 2–5 s. If the initial diffraction pattern shows strong diffraction to high resolution (**Fig. 7c**), a full data set should be collected from that crystal.

27| To collect a full data set, bring the microscope back into focus mode and retract the beam stop. Tilt the stage to the starting angle of data collection to make sure that the crystal remains inside the SA aperture at the high tilt angle and that there are no issues with collecting data while tilted (e.g., no other crystals or grid bars moving into the field of view).

28| Insert the beam stop again, blank the beam and put the microscope into exposure mode.

29| Set up the detector for data collection. To do this, enable the rolling-shutter mode on the TVIPS CMOS TemCam-F416 and set the exposure time for each frame. In rolling shutter mode, each frame is generally collected over a time of 3–6 s depending on the sample.

30| Ensure that crucial parameters such as stage rotation rate, direction of rotation, exposure time and detector distance are recorded before data collection begins. Note that many of these parameters can be deduced from information written directly to the image headers (**Box 4**).

31| Data are collected as the stage is constantly rotated (**Box 1**) while the camera collects continuously[28].
To begin data collection, ensure that the beam is blanked and start the rotation of the stage at a slow and constant rate (~0.1–0.3° per second is typically used). Once the stage has begun to rotate, unblank the beam and begin recording on the detector. Each diffraction data set, consisting of 70–150 images, takes ~5–10 min to complete.

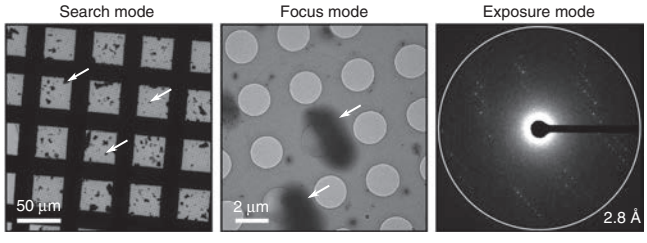

Figure 7 | Example images from search, focus and exposure modes from a model MicroED sample. Search mode shows many well-separated microcrystals across a large area of the grid. White arrows are pointing to a few example microcrystals. When Focus mode is used to search at higher magnification, individual microcrystals, indicated by white arrows, can be located and centered for data collection. The high-quality initial diffraction pattern taken in exposure mode shows a single lattice with tight well-separated spots, indicating that a complete rotation data set should be collected from this crystal.

Box 4 | Recording experimental parameters in diffraction image metadata

Subsequent data processing requires the relative tilt angle and tilt range to be known for each recorded diffraction image. By default, the data acquisition system may not provide this information in the metadata that is included in the output images. We use in-house-developed software, which has been made publicly available (http://cryoem.janelia.org/pages/MicroED—the tool converts TVIPS image format to a format that the image processing software can understand: i.e., SMV), to supplement the image metadata with the tilt angle periodically polled from the electron microscope. The tilt direction is determined by comparing the difference in tilt angle between consecutive frames. Because polling and image acquisition are asynchronous, the relative tilt angle of each frame is then calculated from the calibrated tilt rate and the timestamp of the frame (see Hattne *et al.*[29] for more detail; this article is open access and can be found here: http://journals.iucr.org/a/issues/2015/04/00/mq5031/index.html).

32| Because radiation damage will eventually reduce the diffracting power of the crystals, it may be necessary to merge data from multiple crystals. Therefore, it is recommended that when a grid has well-diffracting crystals, as many quality data sets should be collected from it as possible. When the data collection session is complete, transfer all data from the microscope or camera computer. Center the stage and remove the cryo-holder. Finally, if no other samples are to be loaded for the day, start the cryo-cycle on the TEM.

? TROUBLESHOOTING

Troubleshooting help for common issues in MicroED sample preparation and data collection can be found in **Table 1**.

TABLE 1 | Troubleshooting table.

Problem	Possible reason	Solution
Beam not visible	Column valves and/or cryo-holder shutter are closed	Ensure that the column values and the cryo-holder shutter are in the open position
	Beam is off-center	Slightly retract the holder and check the beam; if it is off-center, re-align the beam
	Blotting is inadequate and ice is too thick	Increase the blotting time or reduce the volume added to the grid surface (Step 10)
Poor contrast	Blotting is inadequate and ice is too thick	Increase blotting time or reduce the volume added to the grid surface (Step 10)
	Crystal mother liquor is too dense	Dilute the crystallization solution to lower the concentration of dense components (e.g., glycerol and high-molecular-weight PEGs)
Low crystal density on the grid	Concentration of crystals is low	Use crystal drops with heavy granular aggregates
	Crystals do not remain on the carbon surface during blotting	Apply crystal solution to both sides of the TEM grid during blotting with a plunge-freezing device
		Try manual blotting and add a larger volume of sample
		Different glow-discharge settings may be used to alter the carbon surface chemistry (Step 9)
Salt crystals on grid	High salt in crystal mother liquor	Attempt to dilute the salt in the sample buffer if the crystals are stable
	Excessive evaporation of crystal solution	Reduce the time the crystal solution is exposed to the air to decrease evaporation and salt crystallization
		Add crystal solution to grid while in the humidified Vitrobot chamber
Weak diffraction	Crystals not preserved during freezing	Test different concentrations of cryo-protectants (e.g., 10% ethylene glycol) and different blotting times
	Beam intensity is too low	Increase the dose rate during exposure or increase the exposure time
	Crystals are not well-ordered	Optimize crystallization conditions
	Exposure time is too short	Increase exposure time
	Rotation rate is too fast	Decrease the rotation rate
	Crystal and/or ice too thick	Choose thinner crystal and/or thinner ice area
		Optimize blotting and grid preparation

(continued)

TABLE 1 | Troubleshooting table (continued).

Problem	Possible reason	Solution
Crystal does not survive data collection	Crystals are sensitive to beam-induced damage	Reduce the dose rate until the crystal provides diffraction data across enough frames for downstream processing. After processing, multiple crystals may be merged to improve data completeness
Diffraction spots too close together or overlapping	Unit cell parameters are large, leading to spot overlap	Increase the diffraction length (detector distance) on the microscope. Find a good balance between recording high-resolution reflections and obtaining well-separated spots
	Exposure time is too long, resulting in wide wedges of reciprocal space being sampled and diffraction spots overlapping	Decrease the exposure time
	Rotation rate is too fast, resulting in wide wedges of reciprocal space being sampled and diffraction spots overlapping	Reduce the rotation rate of the stage

ANTICIPATED RESULTS

Ideal grids prepared by this protocol should have a thin layer of ice and easily distinguishable crystals when viewing in low-magnification search mode on the EM (**Fig. 6a**). There should be a high concentration of crystals on the grid, but the crystals should also be spaced far enough apart that multiple crystals will not come into view when the stage is tilted during data collection. When the quality of a microcrystal is being tested by taking an initial exposure, well-ordered microcrystals should produce a high-resolution diffraction pattern, free from split or smeared spots (see example pattern in **Fig. 7c**). Finally, the collected data set should show strong diffraction spots for most frames so that enough of reciprocal space is sampled to allow for subsequent unit cell determination and indexing. We have found that ~10–30° is sufficient for accurate autoindexing with MOSFLM. After data collection described in this protocol, data processing and refinement using standard crystallography programs is the next step toward determining the protein's high-resolution structure.

ACKNOWLEDGMENTS Work in the Gonen lab is supported by the Howard Hughes Medical Institute.

AUTHOR CONTRIBUTIONS D.S., B.L.N. and T.G. wrote the manuscript. D.S., B.L.N., M.J.d.l.C., F.E.R., J.H. and T.G. designed and performed the experiments, and edited the manuscript. J.L. and J.H. worked on software design. D.S., T.G. and S.S. designed and built the rotation controller. G.C. provided Fig. 2d,h. All authors read and approved the manuscript.

COMPETING FINANCIAL INTERESTS The authors declare no competing financial interests.

1. Chapman, H.N. *et al.* Femtosecond X-ray protein nanocrystallography. *Nature* **470**, 73–77 (2011).
2. Moukhametzianov, R. *et al.* Protein crystallography with a micrometre-sized synchrotron-radiation beam. *Acta Crystallogr. D Biol. Crystallogr.* **64**, 158–166 (2008).
3. Nannenga, B.L., Shi, D., Leslie, A.G. & Gonen, T. High-resolution structure determination by continuous-rotation data collection in MicroED. *Nat. Methods* **11**, 927–930 (2014).
4. Shi, D., Nannenga, B.L., Iadanza, M.G. & Gonen, T. Three-dimensional electron crystallography of protein microcrystals. *Elife* **2**, e01345 (2013).
5. Zhang, Y.B. *et al.* Single-crystal structure of a covalent organic framework. *J. Am. Chem. Soc.* **135**, 16336–16339 (2013).
6. Wan, W., Sun, J.L., Su, J., Hovmoller, S. & Zou, X.D. Three-dimensional rotation electron diffraction: software RED for automated data collection and data processing. *J. Appl. Crystallogr.* **46**, 1863–1873 (2013).
7. Mugnaioli, E., Gorelik, T. & Kolb, U. "Ab initio" structure solution from electron diffraction data obtained by a combination of automated diffraction tomography and precession technique. *Ultramicroscopy* **109**, 758–765 (2009).
8. Jiang, J.X. *et al.* Synthesis and structure determination of the hierarchical meso-microporous zeolite ITQ-43. *Science* **333**, 1131–1134 (2011).
9. Gemmi, M., La Placa, M.G.I., Galanis, A.S., Rauch, E.F. & Nicolopoulos, S. Fast electron diffraction tomography. *J. Appl. Crystallogr.* **48**, 718–727 (2015).
10. Nannenga, B.L., Shi, D., Hattne, J., Reyes, F.E. & Gonen, T. Structure of catalase determined by MicroED. *Elife* **3**, e03600 (2014).
11. Rodriguez, J.A. *et al.* Structure of the toxic core of alpha-synuclein from invisible crystals. *Nature* **525**, 486–490 (2015).
12. Yonekura, K., Kato, K., Ogasawara, M., Tomita, M. & Toyoshima, C. Electron crystallography of ultrathin 3D protein crystals: atomic model with charges. *Proc. Natl. Acad. Sci. USA* **112**, 3368–3373 (2015).
13. Liu, W. *et al.* Serial femtosecond crystallography of G protein-coupled receptors. *Science* **342**, 1521–1524 (2013).
14. Sugahara, M. *et al.* Grease matrix as a versatile carrier of proteins for serial crystallography. *Nat. Methods* **12**, 61–63 (2015).
15. Weierstall, U., Spence, J.C. & Doak, R.B. Injector for scattering measurements on fully solvated biospecies. *Rev. Sci. Instrum.* **83**, 035108 (2012).
16. Gonen, T. The collection of high-resolution electron diffraction data. *Methods Mol. Biol.* **955**, 153–169 (2013).
17. Battye, T.G., Kontogiannis, L., Johnson, O., Powell, H.R. & Leslie, A.G. iMOSFLM: a new graphical interface for diffraction-image processing with MOSFLM. *Acta Crystallogr. D Biol. Crystallogr.* **67**, 271–281 (2011).
18. Leslie, A.G.W. & Powell, H.R. Processing diffraction data with MOSFLM. *NATO Sci. Ser.* **245**, 41–51 (2007).
19. Kabsch, W. *XDS*. *Acta Crystallogr. D Biol. Crystallogr.* **66**, 125–132 (2010).
20. Otwinowski, Z. & Minor, W. Processing of X-ray diffraction data collected in oscillation mode. *Methods Enzymol.* **276**, 307–326 (1997).
21. Waterman, D.G. *et al.* The DIALS framework for integration software. *CCP4 Newslett. Protein Crystallogr.* **49**, 16–19 (2013).
22. Brunger, A.T. Version 1.2 of the crystallography and NMR system. *Nat. Protoc.* **2**, 2728–2733 (2007).
23. Brunger, A.T. *et al.* Crystallography & NMR system: a new software suite for macromolecular structure determination. *Acta Crystallogr. D Biol. Crystallogr.* **54**, 905–921 (1998).
24. Adams, P.D. *et al.* PHENIX: a comprehensive Python-based system for macromolecular structure solution. *Acta Crystallogr. D* **66**, 213–221 (2010).

25. Blanc, E. *et al.* Refinement of severely incomplete structures with maximum likelihood in BUSTER-TNT. *Acta Crystallogr. D Biol. Crystallogr.* **60**, 2210–2221 (2004).
26. Sheldrick, G.M. Experimental phasing with SHELXC/D/E: combining chain tracing with density modification. *Acta Crystallogr. D Biol. Crystallogr.* **66**, 479–485 (2010).
27. Winn, M.D. *et al.* Overview of the CCP4 suite and current developments. *Acta Crystallogr. D* **67**, 235–242 (2011).
28. Huang, P.S. *et al.* High thermodynamic stability of parametrically designed helical bundles. *Science* **346**, 481–485 (2014).
29. Hattne, J. *et al.* MicroED data collection and processing. *Acta. Crystallogr. A Found. Adv.* **71**, 353–360 (2015).
30. Nannenga, B.L., Iadanza, M.G., Vollmar, B.S. & Gonen, T. Overview of electron crystallography of membrane proteins: crystallization and screening strategies using negative stain electron microscopy. *Curr. Protoc. Protein Sci.* **Chapter 17**, Unit17.15 (2013).
31. Wampler, R.D. *et al.* Selective detection of protein crystals by second harmonic microscopy. *J. Am. Chem. Soc.* **130**, 14076–14077 (2008).
32. Stevenson, H.P. *et al.* Use of transmission electron microscopy to identify nanocrystals of challenging protein targets. *Proc. Natl. Acad. Sci. USA* **111**, 8470–8475 (2014).
33. Grassucci, R.A., Taylor, D. & Frank, J. Visualization of macromolecular complexes using cryo-electron microscopy with FEI Tecnai transmission electron microscopes. *Nat. Protoc.* **3**, 330–339 (2008).